https://doi.org/10.15407/ufm.22.04.531

V.Z. TURKEVYCH [1,*], Yu.Yu. RUMIANTSEVA [1,], I.O. HNATENKO [1,***], I.O. HLADKYI [2], and Yu.I. SADOVA [1]**

[1] V. Bakul Institute for Superhard Materials of the N.A.S. of Ukraine, 2 Avtozavodska Str., UA-04114 Kyiv, Ukraine

[2] National Technical University of Ukraine 'Igor Sikorsky Kyiv Polytechnic Institute', 37 Prosp. Peremohy, UA-03056 Kyiv, Ukraine

*vturk@ism.kiev.ua, **yrumuanceva@gmail.com, ***gnatenko_i@ukr.net

THERMODYNAMIC CALCULATION OF Fe–N AND Fe–Ga MELTING DIAGRAMS AT PRESSURES FROM 0.1 MPa TO 7 GPa

This paper presents results of melting-diagrams' calculations for the Fe–N and Fe–Ga systems at atmospheric pressure (0.1 MPa) and at high pressures (3, 5 and 7 GPa). Thermodynamic calculations are performed within the models of phenomenological thermodynamics. As shown, the increase of pressure results in destabilization of high-temperature b.c.c.-Fe modification in Fe–N system and stabilization of Fe_4N equilibrium with the liquid phase. In Fe–Ga system, the intermetallic compounds Fe_3Ga, Fe_6Ga_5, Fe_3Ga_4, and $FeGa_3$ retain their stability up to pressure of 7 GPa. The stabilization of Fe_4N equilibrium with the liquid phase at high pressures indicates that the Fe_4N can be a competing phase in the gallium-nitride crystallization from the Fe–Ga–N system melt.

Keywords: Fe–N and Fe–Ga diagrams, high pressures, thermodynamic calculations, ThermoCalc.

1. Introduction: Background of the Problem and Motivation of the Study

The effects of nitrogen on the properties of iron alloys are variable and depend on many factors, such as nitrogen concentration, presence, alloy composition and other factors [1]. The negative effects of nitrogen are

Citation: V.Z. Turkevych, Yu.Yu. Rumiantseva, I.O. Hnatenko, I.O. Hladkyi, and Yu.I. Sadova, Thermodynamic Calculation of Fe–N and Fe–Ga Melting Diagrams at Pressures from 0.1 MPa to 7 GPa, *Progress in Physics of Metals*, **22**, No. 4: 531–538 (2021)

well known, and dominantly appears when its concentration in metal above the solubility limit in solid metal. This creates conditions for nitrogen to be released from the solid solution. The nitrogen deposition from such a solution, during the metal ageing, reduces the plasticity and strength of steel [2].

On the other hand, nitrogen is sometimes a useful alloying element. For instance, by nitrogen doping, can be amplified some steel's functional properties (if it is necessary). Nitrated steel having a layer of ε-phase on the surface, corrosion resistant in water and in atmospheric conditions has an increased hardness [3]. A new class of high-strength nitrogen-alloyed steel resistant to corrosion has recently been developed. Due to the difference in the interaction of carbon and nitrogen atoms with iron atoms, steel has unique physicochemical and operational properties (high strength, plasticity, absolute corrosion resistance, nebulosity). Nitrogen steels are well welded and technologically sound in both the metallurgical and shipbuilding industries, hence, that their research and development remains interesting from both engineering and a scientific point of view [4].

Interest in the high-pressure phases of iron nitride as potential phases of the Earth's nucleus and mantle is due to their discovery in ultra-deep diamonds [5] and the elevated nitrogen concentrations in some iron meteorites. Equally interesting is the persistence of iron nitride in relation to carbides under conditions of excess nitrogen and carbon [6], which suggests the possibility of carbon nitrogen being displaced from iron compounds. Iron nitrides, γ-Fe_4N and γ′-FeN, along with the metastable phase α-$Fe_{16}N_2$, are also known to be of greatest interest to researchers today, *e.g.*, due to discovery of giant ferromagnetism of α-$Fe_{16}N_2$ phase [7] (see also recent review [8] and references therein). This heightened interest has naturally yielded results: iron alloys are known to be widely used to crystallize diamonds under high pressure and temperature conditions [9]. In addition, there has been recent research into the crystallization of other substances (*e.g.*, the crystallization of wide-area semiconductor materials as gallium nitride) under extreme high pressures and temperatures and using the same alloys [10].

All this leads to the need for a better understanding of the iron-gallium-nitrogen system both under atmospheric pressure and under extreme high temperatures and pressures. These facts make it necessary to construct a diagram 'iron–gallium–nitrogen' under extremal pressures (greater than 1 GPa) also. However, in order to construct a ternary diagram, it is necessary, first of all, to construct binary diagrams: Fe–Ga, Fe–N, Ga–N. Since the authors have already made a phase diagram of the Ga–N system in the first approximation in the previous work [11] that this work is devoted to the construction of the diagrams Fe–Ga and Fe–N. It is expected that this will advance the understanding of the Fe–

Ga–N system behaviour. The authors hope, that the results will make it possible to understand, which is necessary for effective GaN crystallization under high temperatures and pressures. We also hope that this will make it possible to not only grow high-quality single crystals by optimizing the p–T-conditions of growing GaN crystals, as well as allow other researchers to solve their materials science problems, which presented above.

2. Methods and Experiments

Analysis of the data published in [12, 13] showed that in the systems 'iron–nitrogen' and 'iron–gallium' there are low and high-temperature modifications of iron with b.c.c. and h.c.p. structures, respectively. However, when temperatures are reduced to some values, f.c.c.-iron modification changes back to b.c.c. structure.

The model with two sublattices was used to describe the Gibbs free energy dependence on the nitrogen concentration in b.c.c., f.c.c. and h.c.p. iron. The isobar-isothermal potential of Fe_4N is represented by the energy formalism of compounds (CEF) [14]. The model of subregular solutions was used to describe the dependence of Gibbs free energy on the nitrogen concentration in liquid iron. The model parameters for calculating the phase diagram of Fe–N and Fe–Ga systems at atmospheric pressure are taken from [15].

High pressures cause an increase in free Gibbs energy for each phase by an amount:

$$\int_0^p V_m^{ph} dp\,, \tag{1}$$

where V_m^{ph} is the molar volume of the phase with Ph. structure.

The bulk modules, their dependence on pressure, thermal expansion coefficients (CTE), the molar volumes for the solids were taken from

Thermodynamic phases' parameters in Fe–N and Fe–Ga systems [12, 13, 18–23]

Phase	Molar volumes, m^3/mole	Bulk modulus, GPa	Pressure derivative of bulk modulus	CTE, K^{-1}
b.c.c.-Fe	$7.05\cdot10^{-6}$	158.8	5.16	$73.0\cdot10^{-6}$
f.c.c.-Fe	$7.00\cdot10^{-6}$	158.8	5.16	$73.0\cdot10^{-6}$
h.c.p.-Fe	$8.15\cdot10^{-6}$	129.9	5.3	$22.9\cdot10^{-6}$
Liquid Fe	$6.80\cdot10^{-6}$	132.4	6.6	$73.0\cdot10^{-6}$
Liquid Ga	$11.85\cdot10^{-6}$	48.0	9.1	$+114\cdot10^{-6}–22\cdot10^{-8}\cdot T$
Fe_4N	$29.00\cdot10^{-6}$	160.0	5.3	$22.9\cdot10^{-6}$
Fe_3Ga	$30.50\cdot10^{-6}$	172.0	6.6	$52.8\cdot10^{-6}$
Fe_6Ga_5	$87.99\cdot10^{-6}$	172.0	6.6	$52.8\cdot10^{-6}$
Fe_3Ga_4	$58.51\cdot10^{-6}$	172.0	6.6	$52.8\cdot10^{-6}$

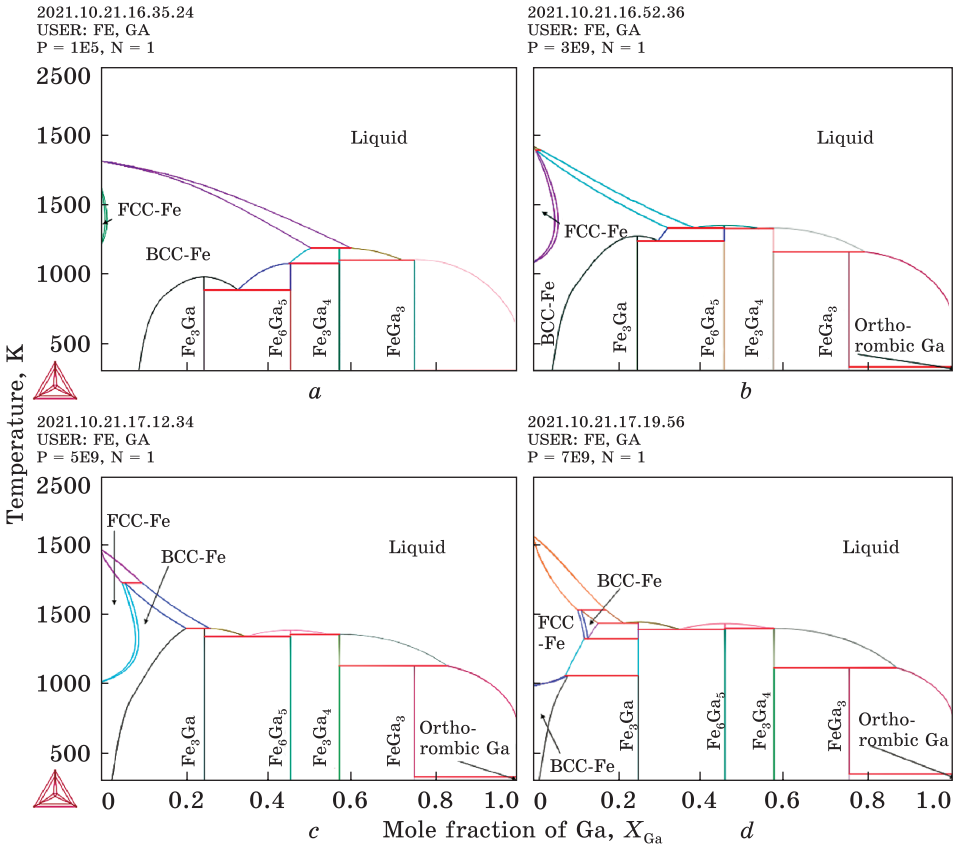

Fig. 1. Phase diagrams of the Ga–N system at 0.1 GPa (*a*), 3 GPa (*b*), 5 GPa (*c*), and 7 GPa (*d*)

the literature summarized in the publication [16]. The liquid phase volume was described in such a way as to minimize deviations from the experimental data. Namely, it is necessary to minimize deviations of the theoretical and experimental data for melting temperatures dependence of h.c.p. iron and Fe_4N on pressure (in [10] Fe_4N was interpreted as Fe_3N).

The pressure dependence of free Gibbs energy is calculated in Murnaghan approximation [17]. Thermodynamic parameters affecting the pressure term of Gibbs free energy for the phases of the Fe–N system are presented in Table.

3. Results and Discussion

Thus, using data from Table 1, after simulating system's behaviour using the ThermoCalc software package [24], the results were obtained, shown in Fig. 1 and Fig. 2.

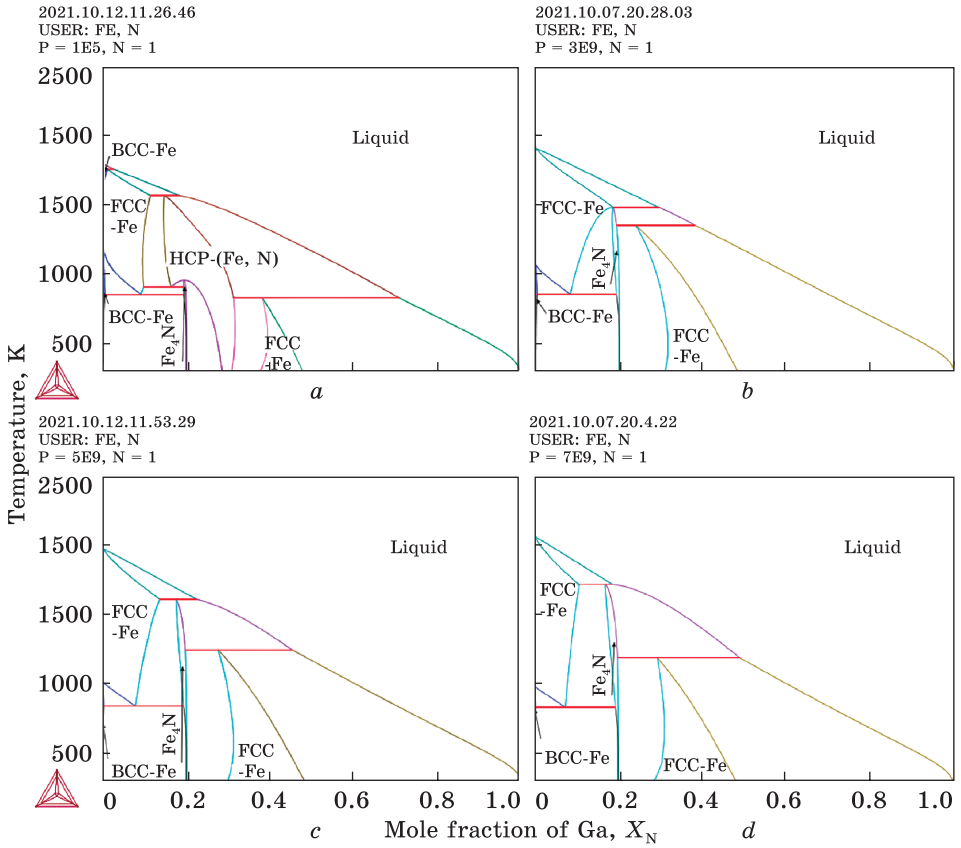

Fig. 2. Phase diagrams of the Fe-N system at 0.1 GPa (*a*), 3 GPa (*b*), 5 GPa (*c*), and 7 GPa (*d*)

The graphs show that the Fe–N phase diagram undergoes next significant changes upon application of pressure:

• the high-temperature modification of b.c.c. iron and the solid-solution nitrogen with iron (h.c.p.-Fe–N) are destabilized;

• the temperature range of Fe_4N existence expands significantly;

• the equilibrium of Fe_4N with the liquid phase is stabilized by the peritectic reaction: $Fe_4N \rightleftarrows$ f.c.c.-iron + liquid.

The topology of the Fe–Ga phase diagram changes insignificantly when pressures are superimposed. Fe_3Ga, Fe_6Ga_5, Fe_3Ga_4 and $FeGa_3$ intermetallic compounds remain stable at pressures up to 7 GPa.

4. Conclusions

The intermetallic compounds Fe_3Ga, Fe_6Ga_5, Fe_3Ga_4 and $FeGa_3$ retain their stability at pressures up to 7 GPa. The stabilization of the equilibrium of Fe_4N with the liquid phase at high pressures indicates that Fe_4N

can be a competing phase in the GaN crystallization from the melt of the Fe–Ga–N system. A similar effect takes place in Fe–Co–C and Fe–Ni–C systems, where cementite is a competing phase of diamond crystallization from solution in the melt [25]. To clarify the situation and possible optimization of the crystallization process of gallium nitride, it is necessary to construct a phase diagram of the Fe–Ga–N system at pressures of 6–7 GPa.

Acknowledgement. This work was supported by the National Research Foundation of Ukraine (NRFU) within the framework of the project 'Gallium Nitride Single Crystals: High Pressure, Structure, Properties' (registrat on number 2020.02/0078) obtained within the NRFU Competition 'Leading and Young Scientists Research Support'.

REFERENCES

1. P.C. Angelo, and B. Ravisankar, *Introduction to Steels: Processing, Properties, and Applications* (CRC Press: 2019).
2. P. Bajaj, A. Hariharan, P. Kürnsteiner, D. Raabe, and E.A. Jägle, *Mater. Sci. Eng.* A, 772 (2020); https://doi.org/10.1016/j.msea.2019.138633
3. W. Qiang, K. Wang, *J. Mater. Process Technol.*, **250**:169 (2017); https://doi.org/10.1016/j.jmatprotec.2017.07.021
4. Z. Brytan, W. Borek, and T. Tański, Introductory Chapter: Why Austenitic Stainless Steels are Continuously Interesting for Science?, *Austenitic Stainless Steels — New Aspects* (IntechOpen: 2017); https://doi.org/10.5772/intechopen.72062
5. Nursultan E. Sagatov, Dinara N. Sagatova, Pavel N. Gavryushkin, and Konstantin D. Litasov, *Crystal Growth & Design* (Article ASAP:2021); https://doi.org/10.1021/acs.cgd.1c00432
6. Bastian K. Brink, Kenny Stehl, Thomas L. Christiansen, and Marcel A.J. Somers, *Journal of Alloys and Compounds*, **690**: 431 (2017); https://doi.org/10.1016/j.jallcom.2016.08.130
7. X. Wang, W.T. Zheng, H.W. Tian, S.S. Yu, W. Xu, S.H. Meng, X.D. He, J.C. Han, C.Q. Sun, and B.K. Tay, *Applied Surface Science*, **220**, Nos. 1–4: 30 (2003); https://doi.org/10.1016/S0169-4332(03)00752-9
8. T.M. Radchenko, O.S. Gatsenko, V.V. Lizunov, and V.A. Tatarenko, *Progress in Physics of Metals*, **21**, No. 4: 580 (2020); https://doi.org/10.15407/ufm.21.04.580
9. Y.N. Palyanov, I.N. Kupriyanov, A.F. Khokhryakov, and Y.M. Borzdov, *Cryst. Eng. Comm.*, **19**, No. 31: 4459 (2017); https://doi.org/10.1039/C7CE01083D
10. I.A. Petrusha, B.S. Sadovyi, P.S. Sadovyi, A.S. Osipov, Yu.Yu. Rumiantseva, P.A. Balabanov, P. Klimczyk, Yu.I. Sadova, O.V. Savitskyi, S.O. Hordieiev, and T.O. Sakal, *Tooling Material Science*, No. 24: 312(2021); https://doi.org/10.333839/2708-731X-2021-24-1-312-325
11. V.Z. Turkevych, Yu.Yu. Rumiantseva, O.V. Savitskyi, S.O. Hordieiev, O.V. Kushch, Yu.I. Sadova, and D.V. Turkevych, *Tooling Material Science*, No. 24: 307(2021); https://doi.org/10.333839/2708-731X-2021-24-1-307-311

12. C. Dasarathy and William Hume-Rothery, *Proceedings of the Royal Society of London. Series A. Mathematical and Physical Sciences*, **286**, No. 1405: 141 (1965); https://doi.org/10.1098/rspa.1965.0135
13. H.A. Wriedt, N.A. Gokcen, and R.H. Nafziger, *Bulletin of Alloy Phase Diagrams,* **8**: 355(1987); https://doi.org/10.1007/BF02869273
14. M. Hillert, *J. Alloys Compd.*, **320**, No. 2: 161 (2001); https://doi.org/10.1016/S0925-8388(00)01481-X
15. P.A. Turchi, L. Kaufman, Z. Liu, and S. Zhou, *Thermodynamics and Kinetics of Phase Transformations in Plutonium Alloys — Part I* (USA: 2004); https://doi.org/10.2172/895082
16. Springer Nature Switzerland AG, Part of Springer Nature [Electronic resource]. — Access mode: https://www.springernature.com/gp/products/journals
17. F.D. Murnaghan, *Proc. Nation. Acad. Sci. USA*, **9**, No. 30: 244 (1944); https://doi.org/10.1073/pnas.30.9.244
18. M. Kusakabe, K. Hirose, R. Sinmyo, Y. Kuwayama, Y. Ohishi, and G. Helffrich, *Journal of Geophysical Research: Solid Earth*, **124**, No. 4: 3448 (2019); https://doi.org/10.1029/2018JB015823
19. M.H. Wetzel, T.T. Rabending, M. Friák, M. Všianská, M. Šob, and A. Leineweber, *Materials*, **14**, No. 14: 3963 (2021); https://doi.org/10.3390/ma14143963
20. Zhi Li, Zhen Zhao, Tong-Tong Shi, and Xi-Min Zang, *International Journal of Modern Physics B*, **34**, No. 17: 2050156 (2020); https://doi.org/10.1142/S0217979220501568
21. A. Leineweber, H. Jacobs, W. Kockelmann, S. Hull, D. Hinz-Hübner, *Journal of Alloys and Compounds*, **384**, Nos. 1–2: 1 (2004); https://doi.org/10.1016/j.jallcom.2004.03.122
22. K.D. Litasov, A. Shatskiy, D.S. Ponomarev, and P.N. Gavryushkin, *Journal of Geophysical Research: Solid Earth*, **122**, No. 5: 3574 (2017); https://doi.org/10.1002/2017JB014059
23. Yukai Zhuang, Xiaowan Su, Nilesh P. Salke, Zhongxun Cui, Qingyang Hu, Dongzhou Zhang, and Jin Liu, *Geoscience Frontiers*,**12**, No. 2: 983 (2021); https://doi.org/10.1016/j.gsf.2020.04.012
24. J.-O. Andersson, Thomas Helander, Lars Hцglund, Pingfang Shi, and Bo Sundman, *Calphad*, **26**, No. 2: 273 (2002); https://doi.org/10.1016/S0364-5916(02)00037-8
25. Y. Bataleva, Y. Palyanov, Y. Borzdov, I. Novoselov, and O. Bayukov, *Minerals*, **8**, No. 11: 522 (2018); https://doi.org/10.3390/min8110522

Received 04.11.2021;
in final version, 17.11.2021

В.З. Туркевич[1], *Ю.Ю. Румянцева*[1],
І.О. Гнатенко[1], *І.О. Гладкий*[2], *Ю.И. Садова*[1]

[1] Інститут надтвердих матеріалів ім. В.М. Бакуля НАН України, вул. Автозаводська, 2, 04114 Київ, Україна

[2] Національний технічний університет України «Київський політехнічний інститут імені Ігоря Сікорського», проспект Перемоги, 37, 03056 Київ, Україна

ТЕРМОДИНАМІЧНИЙ РОЗРАХУНОК ДІАГРАМ ТОПЛЕННЯ Fe–N і Fe–Ga ЗА ТИСКІВ ВІД 0,1 МПа ДО 7 ГПа

В межах моделей феноменологічної термодинаміки виконано розрахунок фазових діаграм систем Fe–N і Fe–Ga за атмосферного тиску (0,1 МПа) та за високих тисків (3, 5 і 7 ГПа). Показано, що підвищення тиску призводить до дестабілізації високотемпературної модифікації ОЦК-Fe в системі Fe–N і стабілізації рівноваги Fe_4N із рідкою фазою. В системі Fe–Ga інтерметаліди Fe_3Ga, Fe_6Ga_5, Fe_3Ga_4 та $FeGa_3$ зберігають свою стабільність за тисків до 7 ГПа. Стабілізація рівноваги Fe_4N з рідкою фазою за високих тисків вказує на те, що Fe_4N може бути конкурувальною фазою за кристалізації нітриду Ґалію з розтопу системи Fe–Ga–N.

Ключові слова: Fe–N, Fe–Ga, високі тиски, термодинамічні розрахунки, ThermoCalc.